BRAIN
A JOURNAL OF NEUROLOGY

Leukoencephalopathy with thalamus and brainstem involvement and high lactate 'LTBL' caused by *EARS2* mutations

Marjan E. Steenweg,[1,*] Daniele Ghezzi,[2,*] Tobias Haack,[3,4] Truus E.M. Abbink,[1] Diego Martinelli,[5] Carola G.M. van Berkel,[1] Annette Bley,[6] Luisa Diogo,[7] Eugenio Grillo,[8] Johann Te Water Naudé,[9] Tim M. Strom,[3,4] Enrico Bertini,[10] Holger Prokisch,[3,4] Marjo S. van der Knaap[1,†] and Massimo Zeviani[2,†]

1 Department of Child Neurology, VU University Medical Centre, De Boelelaan 1117, 1081 HV Amsterdam, The Netherlands
2 Unit of Molecular Neurogenetics, Fondazione Istituto Neurologico 'Carlo Besta', via Temolo 4, 20126 Milan, Italy
3 Institute of Human Genetics, Helmholtz Zentrum München, Ingolstädter Landstrasse 1, D-85764 Neuherberg, Germany
4 Institute of Human Genetics, Technische Universität München, Arcisstrasse 21, 80333 Munich, Germany
5 Department of Pediatrics, Division of Metabolism, Bambino Gesù Children's Hospital, IRCCS, P.za S. Onofrio, 4 00168 Rome, Italy
6 Universitätsklinikum Hamburg-Eppendorf Klinik und Poliklinik für Kinder und Jugendmedizin, Martinistrasse 52, D-20246 Hamburg, Germany
7 Centro de Desenvolvimento Dr Luís Borges, Neuropediatria Hospital Pediátrico de Coimbra, Av. Afonso Romão, Alto da Baleia 3000-602, Coimbra, Portugal
8 Hospital Infantil Joana de Gusmão, Serviço de Neurologia e Neurocirurgia, Rua Rui Barbosa 152, 88025-301 – Florianópolis – SC, Brazil
9 Department of Child Health, Paediatric Neurology Service, University Hospital of Wales, Heath Park, Cardiff, CF14 4XW, UK
10 Department of Neurosciences, Unit of Molecular Medicine for Neuromuscular and Neurodegenerative Disorders, Bambino Gesu' Children's Hospital, IRCCS, Plaza S. Onofrio 4, 00168 Rome, Italy

*,†These authors contributed equally to this work.

Correspondence to:
Marjo S. van der Knaap
Department of Child Neurology, VU University Medical Centre, De Boelelaan 1117, 1081 HV Amsterdam, The Netherlands
E-mail: ms.vanderknaap@vumc.nl

or

Massimo Zeviani
Unit of Molecular Neurogenetics, Fondazione Istituto Neurologico 'Carlo Besta', via Temolo 4, 20126 Milan, Italy
E-mail: zeviani@istituto-besta.it

In the large group of genetically undetermined infantile-onset mitochondrial encephalopathies, multiple defects of mitochondrial DNA-related respiratory-chain complexes constitute a frequent biochemical signature. In order to identify responsible genes, we used exome-next-generation sequencing in a selected cohort of patients with this biochemical signature. In an isolated patient, we found two mutant alleles for *EARS2*, the gene encoding mitochondrial glutamyl–tRNA synthetase. The brain magnetic resonance imaging of this patient was hallmarked by extensive symmetrical cerebral white matter abnormalities sparing the periventricular rim and symmetrical signal abnormalities of the thalami, midbrain, pons, medulla oblongata and cerebellar white matter. Proton magnetic resonance spectroscopy showed increased lactate. We matched this magnetic resonance imaging pattern with that of a cohort of 11 previously selected unrelated cases. We found mutations in the *EARS2* gene in all. Subsequent detailed clinical and magnetic resonance imaging based phenotyping revealed two distinct groups: mild and severe. All 12 patients shared an infantile onset and rapidly progressive disease with severe magnetic resonance imaging abnormalities and increased lactate in body fluids

and proton magnetic resonance spectroscopy. Patients in the 'mild' group partially recovered and regained milestones in the following years with striking magnetic resonance imaging improvement and declining lactate levels, whereas those of the 'severe' group were characterized by clinical stagnation, brain atrophy on magnetic resonance imaging and persistent lactate increases. This new neurological disease, early-onset leukoencephalopathy with thalamus and brainstem involvement and high lactate, is hallmarked by unique magnetic resonance imaging features, defined by a peculiar biphasic clinical course and caused by mutations in a single gene, *EARS2*, expanding the list of medically relevant defects of mitochondrial DNA translation.

Introduction

Mitochondria are the major powerhouse of the cell, generating heat and most ATP, the common energy currency for endoergonic metabolic reactions. ATP is synthesized through the process of oxidative phosphorylation, carried out by the mitochondrial respiratory chain. The mitochondrial respiratory chain is composed of five multi-heteromeric complexes located in the mitochondrial inner membrane. Mitochondria have their own DNA, a 16.5-kb circular molecule, encoding 13 essential mitochondrial respiratory chain proteins. The maintenance and expression of mitochondrial DNA, including replication, transcription and translation, is dependent on systems encoded by nuclear DNA genes. Mutations of mitochondrial DNA and of the vast repertoire of nuclear genes converging on the formation and function of mitochondrial respiratory chain are responsible for mitochondrial disorders, a heterogeneous group of conditions characterized by mitochondrial respiratory chain dysfunction. While analysis of mitochondrial DNA is well standardized and mitochondrial DNA-related disorders are relatively well characterized, the list of nuclear genes associated with mitochondrial dysfunction is constantly increasing and many still await discovery (Ghezzi and Zeviani, 2011). The advent of next-generation sequencing technology facilitates the identification of new disease loci in small groups of patients, single families and even single patients, and is expected to transform routine clinical diagnosis (Haack *et al.*, 2010).

We exploited unbiased exome-next-generation sequencing to discover mutations in *EARS2* in a single baby boy affected by an early-onset mitochondrial leukoencephalopathy. This gene encodes the mitochondrial aminoacyl–tRNA synthetase (ARS) specific for glutamate (E), an enzyme involved in mitochondrial DNA translation. The MRI features of this patient matched with those of a cohort of 11 *a priori* selected patients (Steenweg *et al.*, in press). *EARS2* sequence analysis revealed different mutations in each and every patient of this cohort, thus defining a specific clinical, neuroimaging and genetic entity.

Materials and methods

Informed consent for participation in this study was obtained from the parents of all patients, in agreement with the Declaration of Helsinki and approved by the Ethical Committees of the Fondazione Istituto Neurologico–IRCCS, Milan, Italy and of the VU University Medical Centre, Amsterdam, The Netherlands.

Exome sequencing

Exonic sequences of our index patient were enriched by using the SureSelect Human All Exon 50 Mb kit (Agilent), and subsequently sequenced as 76 paired-end runs on a Genome Analyzer IIx system (Illumina) to an average 110-fold coverage. Read alignment to the human genome assembly hg19 was performed with BWA (v 0.5.8). Small insertions and deletions and single-nucleotide variants were detected with SAMtools (v 0.1.7).

Mutation screening

Genomic DNA was extracted by standard methods. The nine exons and intron–exon junctions of the human *EARS2* gene were polymerase chain reaction amplified using suitable primers (available upon request); and analysed by Sanger sequencing.

Biochemical assays

Supernatants of $800 \times g$ muscle homogenates or digitonin-treated cultured skin fibroblasts were used to measure the activities of mitochondrial respiratory chain complexes and citrate synthase (Bugiani *et al.*, 2004). Oxygen consumption rate and extra-cellular acidification rate were measured in a SeaHorse FX-96 apparatus (Wu *et al.*, 2007), as detailed in the Supplementary material.

Miscellaneous

Muscle biopsies were processed according to standard histological and histochemical techniques (Heckmatt and Dubowitz 1984; Sciacco and Bonilla, 1996).

Results

Case report

The index patient, Patient 1, is a 6-year-old boy, born at 40 weeks of gestation after an uneventful pregnancy; the only child of healthy Italian unrelated parents. Weight, height and head circumference were normal at birth. Hypotonia was noted at 1 month.

At 3 months he was alert but failed to achieve head control. Laboratory investigations at 4 months revealed intermittent elevations of serum transaminases (up to $5\times$), α-fetoprotein (804 ng/ml, normal < 10), and lactate (6.5 mM, normal < 2). Brain MRI at 5 months revealed symmetrical swelling and T_2 hyperintensity of the thalami, hypothalami, midbrain, pons, medulla oblongata and cerebellar white matter (Supplementary Fig. 1). The posterior part of the corpus callosum was abnormally thin. In normal 5-month-old infants the cerebral white matter is still largely unmyelinated, resulting in mild T_2-hyperintensity. In the index patient, however, large parts of the cerebral white matter had a higher signal intensity, indicating lesion. Notably, a periventricular rim was spared and had a normal T_2 signal (Supplementary Fig. 1). Proton magnetic resonance spectroscopy of the cerebral white matter showed increased lactate (Supplementary Fig. 1). At 6 months, he manifested drug-refractory seizures, which relapsed at 3 years. Now, at age 6 years he is seizure-free without medication. During a 4-year follow-up, he never achieved head and postural control. He can swallow but cannot chew, has spastic tetraparesis, dystonia, bradykinesia, bilateral ptosis and ophthalmoplegia, severe visual defect and absence of speech.

Muscle light microscopy showed cytochrome *c* oxidase (COX) negative, succinate dehydrogenase dark blue fibres (Supplementary Fig. 1). Complex I, III and IV activities were reduced in muscle, whereas succinate dehydrogenase and Complex V were normal. The same assays in fibroblasts showed milder reduction of Complex III and Complex IV activities (Supplementary Table 1). SeaHorse-based microscale oxygraphy on fibroblasts revealed reduction of maximal respiratory rate, and reduced oxygen consumption rate to extra-cellular acidification rate ratio, reflecting increased production of lactate (Fig. 1A and B). Sanger sequence analysis ruled out the presence of pathogenic mutations in mitochondrial DNA and in several oxidative phosphorylation-related nuclear genes.

Exome–next-generation sequencing analysis

To prioritize candidate disease genes, we step-wise filtered the raw data, as summarized in Supplementary Table 2. Since combined oxidative phosphorylation defects are rare and severe conditions, we expected causal variants to alter the amino acid sequence and have a frequency <0.5% in available single-nucleotide polymorphism databases. Based on a recessive pattern of inheritance, we then filtered for genes carrying compound heterozygous or homozygous rare variants. Under the hypothesis of a mitochondrial disorder, we focused on genes encoding proteins with
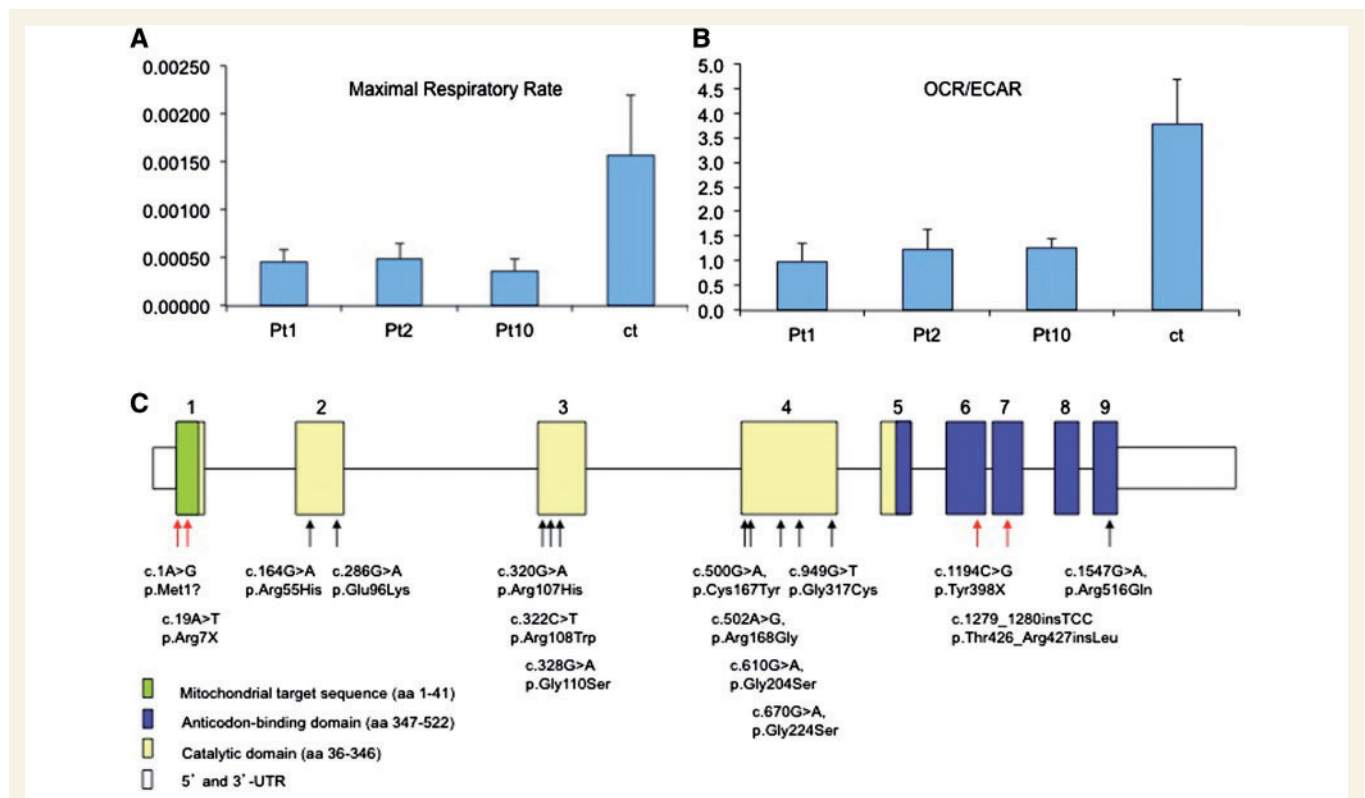

Figure 1 (**A**) Maximal respiration rate measured in fibroblasts from Patients (Pt) 1, 2 and 9 and a control subject (C_t). (**B**) Ratio between oxygen consumption rate (OCR) and extra-cellular acidification rate (ECAR), in fibroblasts from Patients 1, 2 and 9 and a control subject. (**C**) Schematic representation of *EARS2* gene, with mutations identified in this study. Functional domains of the EARS2 protein are in colour. Red arrows indicate mutations that prevent the synthesis or cause the premature truncation of the EARS2 protein, therefore predicting the loss of its function.

Table 1 *EARS2* mutations

Patient	Number	Country of origin	DNA	Exon	Protein	Father/mother
1		Italy	c.502A > G	4	p.Arg168Gly	M
			c.1279_1280insTCC	7	p.Thr426_Arg427insLeu	M
			c.322C > T	3	p.Arg108Trp	F
2	mito21	Belgium	c.322C > T	3	p.Arg108Trp	F
			c.1194C > G	6	p.Tyr398X	M
3	mito10	UK	c.322C > T	3	p.Arg108Trp	M
			c.328G > A	3	p.Gly110Ser	F
4	mito11	USA	c.328G > A	3	p.Gly110Ser	n.a.
			c.610G > A	4	p.Gly204Ser	n.a.
5	mito12	Belgium	c.286G > A	2	p.Glu96Lys	F
			c.500G > A	4	p.Cys167Tyr	M
6	mito1	Israel	c.322C > T	3	p.Arg108Trp	M
			c.949G > T	4	p.Gly317Cys	F
7	mito72	Switzerland	c.164G > A	2	p.Arg55His	F
			c.670G > A	4	p.Gly224Ser	M
8	mito90	Portugal	c.1A > G	1	p.Met1?	M
			c.320G > A	3	p.Arg107His	F
9	mito99	Germany	c.322C > T	3	p.Arg108Trp	F
			c.1547G > A	9	p.Arg516Gln	M
10	mito104	UK	c.19A > T	1	p.Arg7X	F
			c.322C > T	3	p.Arg108Trp	M
11, 12	mito120, mito121	Brazil	c.286G > A	2	p.Glu96Lys	F
			c.500G > A	4	p.Cys167Tyr	M

Nomenclature according to HGVS (http://www.hgvs.org/mutnomen). n.a = not available; F = father; M = mother.

confirmed or predicted mitochondrial localization corresponding to a MitoP2 SVM score >1. This approach selected a single mutant gene, *EARS2*, encoding mitochondrial glutamyl–tRNA synthetase. The maternal allele harboured two mutations: a missense c.502A > G transition, predicting a p.Arg168Gly change, and a c.1279_1280insTCC, predicting the insertion of a Leu residue, p.Thr426_Arg427insLeu. The paternal allele harboured a c.322C > T transition, predicting a p.Arg108Trp change. Both parents were heterozygous for the corresponding alleles (Table 1 and Fig. 1C).

Magnetic resonance imaging pattern recognition

In order to confirm the pathogenic role of the *EARS2* mutations, we searched for similar cases by comparing the MRI pattern of Patient 1 with those defined in the Amsterdam leukoencephalopathy database, which contains the MRIs of more than 3000 cases with a leukoencephalopathy of unknown origin. These data are systematically analysed and categorized into patterns that define novel MRI phenotypes (Van der Knaap *et al.*, 1999). When matching with a consistent clinical phenotype, a disease entity is assumed and further studies are initiated.

In the context of this database, several patients were identified over the last 10 years, who presented with neurological deterioration in the first year of life and an MRI pattern similar to that of Patient 1 (Fig. 2A–C). Signal abnormality and swelling of the deep cerebral white matter was associated with consistent sparing of the periventricular rim. The corpus callosum, thalamus, basal ganglia, midbrain, pons, medulla oblongata and cerebellar white matter were also consistently affected. In five patients, the posterior part of the corpus callosum was abnormally thin (Fig. 3). Proton magnetic resonance spectroscopy of the abnormal white matter revealed elevated lactate. However, MRI features showed striking improvement from the second year on (Fig. 2D–F) and lactate in proton magnetic resonance spectroscopy became normal. This disease-associated MRI pattern was recently proposed as a possible mitochondrial defect in seven patients (Steenweg *et al.*, in press). Reassessment of the database now revealed the presence of nine such patients; DNA of eight were available and their MRI details are summarized in Supplementary Table 3 (Patients 2–8 and 12).

The database revealed a second group of three patients, who had a similar but more severe MRI pattern, summarized in Supplementary Table 3 (Patients 9–11). The cerebral white matter was more diffusely abnormal and more severely swollen than in the first group, but a thin periventricular rim was consistently spared (Fig. 4A–C). These three patients had a dysplastic corpus callosum with agenesis of the posterior part (Fig. 3); as a consequence, the lateral ventricles had an abnormal, parallel position. Proton magentic resonance spectroscopy revealed elevated lactate. Two patients had follow-up MRIs, which revealed progressive atrophy of affected structures, including severe bilateral thinning of the cerebral mantle and thalami (Fig. 4D–F). Interestingly, the older brother of Patient 11, Patient 12 (Supplementary Table 3), belongs to the first group, with only focal, mild remaining signal abnormalities within the deep cerebral white matter and no dysgenesis of the corpus callosum.
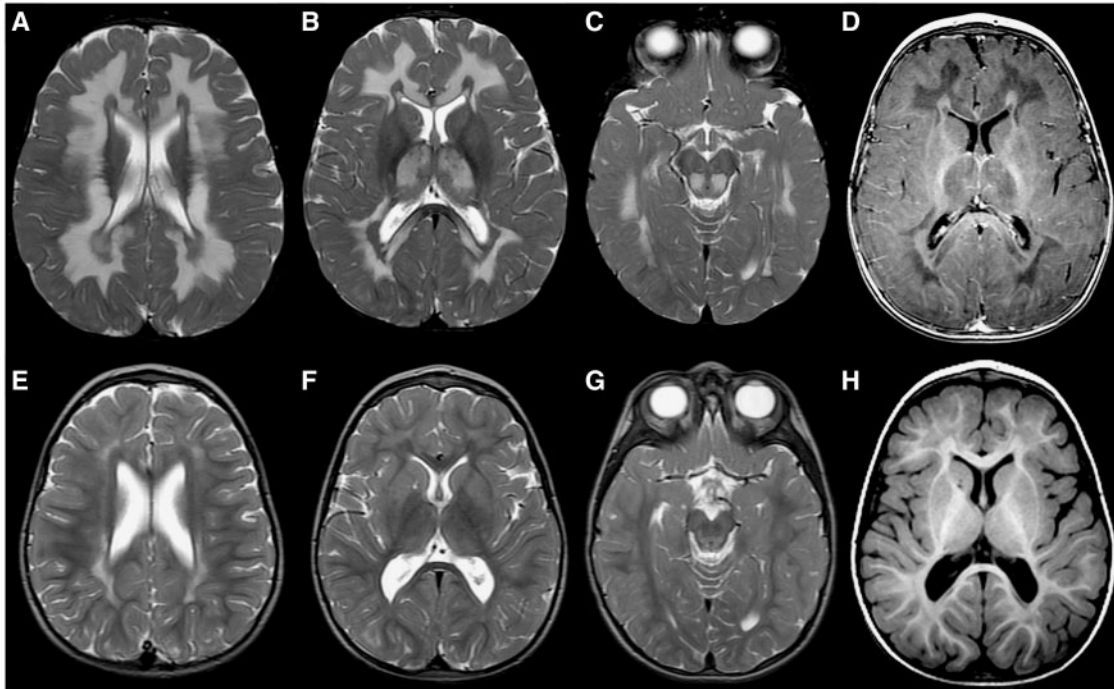
Figure 2 Axial T_2- (**A–C** and **E–G**) and T_1-weighted images (**D** and **H**) in Patient 6 at 11 months (**A–D**) and 3 years (**E–H**). Note the extensive T_2-hyperintense and T_1-hypointense signal of the deep cerebral white matter with sparing of a periventricular rim (**A**, **B** and **D**). There are also signal abnormalities in the thalami (**B**) and dorsal part of the midbrain (**C**). Note the impressive improvement 2 years later (**E–H**).
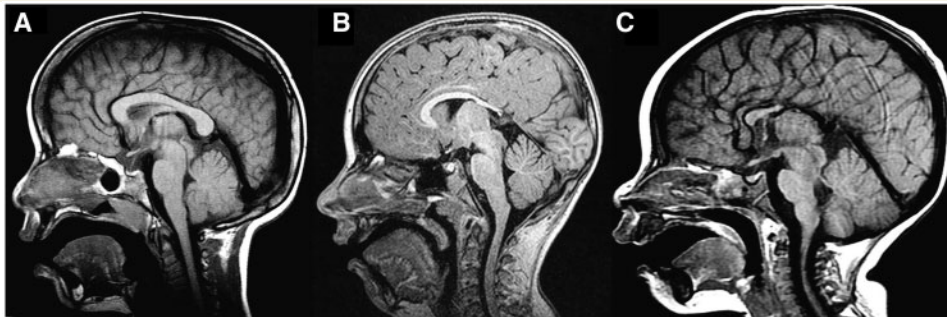

Figure 3 Sagittal T_1-weighted images in Patients 4 (**A**), 2 (**B**) and 11 (**C**). In Patient 4, the corpus callosum is normal (**A**). In Patient 2, the posterior part of the corpus callosum is abnormally thin (**B**). In Patient 11, the corpus callosum development is incomplete and the posterior part is lacking (**C**).

EARS2 mutational analysis

We sequenced the exons and intron–exon boundaries of the *EARS2* gene in Patients 2–12 and their parents. In each and every patient, we found compound heterozygous allelic mutations of the gene (Table 1). Similar to the mutations found in Patient 1, the additional mutations of our cohort are either absent or present at a frequency of <0.03% in cumulative genomic data from our in-house database, containing 819 genomes from Europeans (1638 alleles), and in the public single nucleotide polymorphism databases, including dbSNP (http://www.ncbi.nlm.nih.gov/projects/SNP) and EVS (http://evs.gs.washington.edu/EVS), which altogether contain approximately 12 000 alleles. The only exception is mutation p.Gly224Ser, found in one allele of Patient 7, which is present in 0.23% of database-stored alleles. When analysed by *ad hoc* software for pathogenicity prediction these mutations scored high or very high for likelihood to be deleterious (Supplementary Table 4). In our index case, Patient 1, the two maternal mutations were both absent in the available databases, whereas the paternal c.322C > T change was found in 3 out of approximately 13 500 alleles. This mutation was also found in four additional alleles of our cohort, harboured by Patients 2, 3, 6, 9
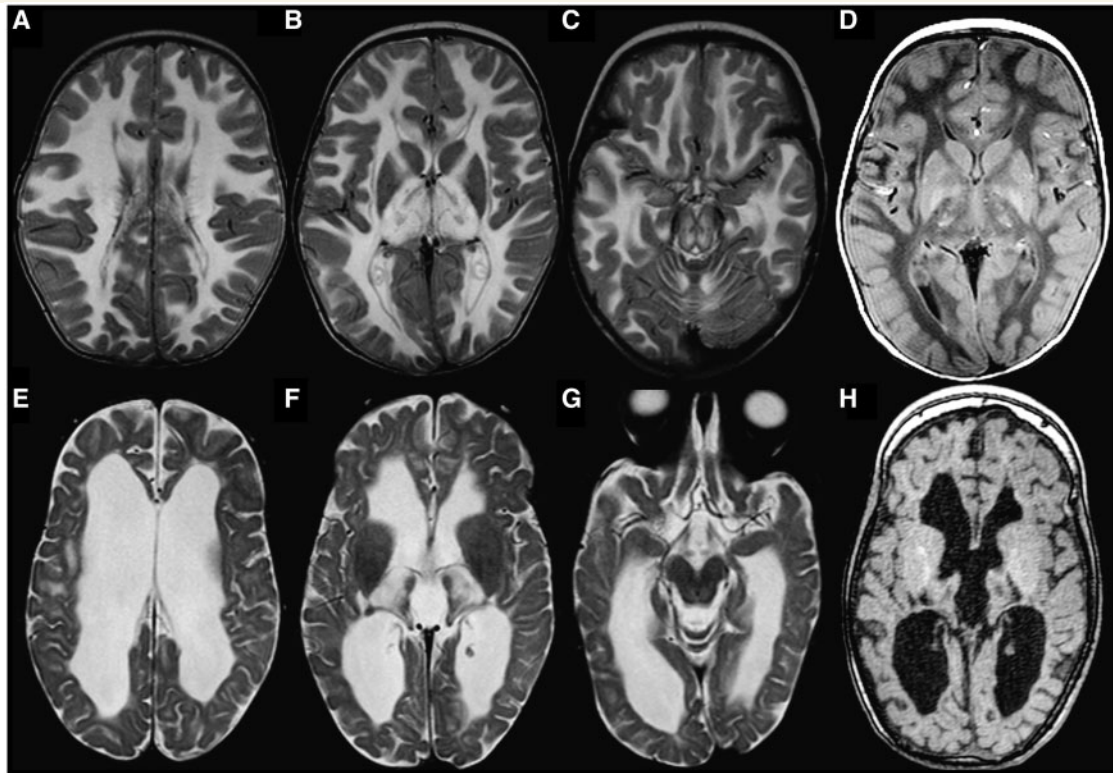
Figure 4 Axial T_2- (**A–C** and **E–G**) and T_1-weighted images (**D** and **H**) in Patient 9 at 8 months (**A–D**) and 4 years (**E–H**). Note the diffuse T_2-hyperintense and T_1-hypointense signal of the cerebral white matter, only sparing a periventricular rim (**A**, **B** and **D**). There are also signal abnormalities in the thalami (**B**) and the midbrain (**C**). Three years later there is serious atrophy of the cerebral white matter and thalami (**D**, **E** and **H**). The midbrain signal abnormalities have disappeared (**F**).

and 10. Taken together, our results indicate that these mutations are rare, or extremely rare, non-polymorphic variants, likely or certainly deleterious, in agreement with a pathogenic role for a recessive trait.

Clinical and biochemical phenotypes

Clinically, our patients fall in two groups, severe and mild (Supplementary Table 5), according to their disease course and reflecting the MRI pattern (Supplementary Table 3). In the severe group, comprising Patients 1 and 9–11, lack of psychomotor development and hypotonia were observed soon after birth, followed by spastic tetraparesis, dystonia, visual impairment and seizures. Patients later stabilized, but failed to improve, remaining severely disabled and eventually tube-fed. The patients of this group had persistent lactate elevations in body fluids and proton magnetic resonance spectroscopy of the brain (Supplementary Table 6). In the mild group, comprising Patients 2–8 and 12, early development was normal or mildly delayed. The clinical onset occurred later, most often in the second half of the first year of life, with clinical regression characterized by spasticity, loss of milestones and sometimes seizures and extreme irritability. Lactate was high in blood and CSF (Supplementary Table 6; for levels see Steenweg *et al.*, in press). From the second year on, clinical and biochemical improvement occurred

with matching MRI improvement. Lactate in body fluids and proton magentic resonance spectroscopy of the brain declined (Supplementary Table 6; for levels see Steenweg *et al.*, in press). All patients regained milestones, including walking with or without support in most. Seizures were attenuated and eventually disappeared and spasticity improved. So far, no second episode of regression has occurred in any (Steenweg *et al.*, in press).

Biochemical assays of individual mitochondrial respiratory chain complexes in cultured fibroblasts ranged from moderate, combined reduction of mitochondrial respiratory chain activities, as in the index case, Patient 1, to hardly any detectable defect in others (Steenweg *et al.*, in press). However, a consistent biochemical phenotype emerged by measuring the overall respiratory capacity in three cultured cell lines (Fig. 1A and B): one belonging to a patient with mild clinical course (Patient 2) and two to patients with the severe presentation (Patients 1 and 9). The detection of reduced oxygen consumption rate and increased lactate production is likely to depend on, and reflects, the cumulative impairment of respiration by the whole set of mitochondrial respiratory chain complexes.

Discussion

By integrating the information obtained from exome-next-generation sequencing and *ad hoc* gene filtering in a single

index case with systematic MRI pattern recognition in patients with unclassified leukoencephalopathies, we identified a series of 12 subjects sharing a set of common features, including: (i) mutations in the same gene; (ii) similar cardinal neuroimaging (MRI) characteristics; and (iii) a well-defined clinical syndrome, variations of which corresponded to the severity of the MRI phenotypes. These results provide evidence for the existence of a new specific mitochondrial disease condition: leukoencephalopathy with thalamus and brainstem involvement, and high lactate, 'LTBL'.

Patient 1 was diagnosed to have a mitochondrial disease, based on biochemical and morphological signatures indicating oxidative phosphorylation impairment in muscle and fibroblasts. Exome-next-generation sequencing screening and *ad hoc* filtering against known or predicted mitochondrial gene products revealed allelic mutations in a single gene, *EARS2*, encoding mitochondrial glutamyl–aminoacyl tRNA synthetase, an essential component of the mitochondrial DNA-specific protein-synthesis machinery. The mutations were considered as likely deleterious by *in silico* analysis, but the definite demonstration of their pathogenic role was provided by the identification of numerous additional mutations in the same gene in a cohort of unrelated patients selected on the basis of common key neuroimaging features. The discovery of different, rare or unique, non-synonymous, potentially deleterious, changes in unrelated subjects with similar phenotypic traits is the gold standard to demonstrate genotype–phenotype causality.

The effectiveness of this integrated procedure in the present study supports the idea that the combination of powerful technology with systematic interpretation of clinical and morphological observations can work synergistically to elucidate the aetiological fundaments of mitochondrial disorders.

The common MRI pattern of our patients was associated with a consistent neurological syndrome, characterized by regression in the first year of life. Most patients displayed some developmental delay prior to the onset of overt, rapid neurological deterioration. Interestingly, this downhill phase, mainly characterized by spasticity, was followed by stabilization, improvement and partial regain of lost skills, although most patients had residual spasticity. A smaller group of patients, including the index case, had a more severe presentation with a very early onset of neurological impairment, at birth or soon afterwards. However, this group of severely affected patients also displayed clinical stabilization over time. This bi-phasic clinical course indicates a single hit early in life, followed by stabilization. The occurrence and extent of recovery most likely depend on the severity of brain damage caused by the first episode. If damage is severe and irreversible, brain atrophy ensues, associated with severe permanent handicap. If cellular impairment is compatible with substantial nerve cell survival and recovery, further brain development and maturation occurs, leading to clinical improvement. These data suggest that *EARS2* mutations particularly affect brain development. This hypothesis is reinforced by dysgenesis of the corpus callosum, detected in the most severely affected patients.

Our study raises a number of other questions. The pathophysiological mechanisms underlying the clinical and MRI features of *EARS2*-associated LTBL are unclear. In spite of severe clinical

impairment and brain abnormalities, and malfunctioning of an essential component of a crucial mitochondrial pathway our patients showed inconsistent biochemical alterations, indicating partial preservation of functional proficiency of the mutant enzyme. Mutations in other mitochondrial ARSs, for instance *DARS2* and *RARS2*, show the same biochemical inconsistency, suggesting that this is a general phenomenon (Edvarson *et al.*, 2007; Scheper *et al.*, 2007). Our working hypothesis is that in mitochondrial DNA translation defects, particularly those involving mitochondrial ARSs, the window for disease manifestation is narrow. This pathway is essential for life, so that most mutations are either too drastic to allow extrauterine survival, or too mild to produce a phenotype. As a consequence, affected individuals are rare and display a selected group of permissive mutations. This hypothesis can also provide a clue to explain the intriguing observation that each and every case of our cohort of affected individuals was compound heterozygous for *EARS2* mutations, usually combining a predictably severe change, for instance, a nonsense mutation or a clearly deleterious amino acid substitution, e.g. p.Met1?, with predictably milder mutations, for instance a missense mutation in moderately conserved domains or a conservative amino acid change (Table 1 and Supplementary Table 4). Interestingly, similar molecular genetic signatures, i.e. lack of homozygous or compound heterozygous loss-of-function mutations, and predominant combination of drastic plus milder changes, occur also in patients with mutant *DARS2* and *RARS2* (Edvarson *et al.*, 2007; Scheper *et al.*, 2007), suggesting that this narrow permissive window can be a general condition, underlying a common pathophysiological mechanism in mutations of different mitochondrial ARSs.

An intriguing clinical observation is that, in contrast to the extreme and haphazard clinical heterogeneity of many mitochondrial disorders, mutations of genes encoding mitochondrial ARSs are usually associated with specific clinical syndromes: for instance, leukoencephalopathy with brainstem and spinal cord involvement and high lactate (LBSL) in *DARS2* mutations (>40 published cases, OMIM 610956); pontocerebellar hypoplasia type 6 (PCHD-6) in *RARS2* mutations (seven published cases, OMIM 611524), and LTBL associated with *EARS2* mutations. This seems to be the case also for other, rarer mutant mitochondrial ARSs, although the frequency is too low to provide definite evidence for conditions associated with mutations in *YARS2* (Riley *et al.*, 2010); *HARS2* (Pierce *et al.*, 2011); *AARS2* (Götz *et al.*, 2011); and *SARS2* (Belostotsky *et al.*, 2011). The mechanisms underpinning these specific clinical–genetic associations are presently unknown.

In summary, early-onset leukoencephalopathy with thalamus and brainstem involvement and high lactate, LTBL, is a new neurological disease, hallmarked by unique MRI features, defined by a peculiar biphasic clinical course, and caused by mutations in a single gene, *EARS2*, expanding the list of medically relevant defects of mitochondrial DNA translation (Rötig *et al.*, 2011). The MRI pattern appears to offer a more reliable diagnostic clue than standard biochemical workup, and in combination with rather consistent clinical features, delineate a syndrome that is specific enough to target the correct molecular diagnosis.

Acknowledgements

Funding

Supplementary material

Supplementary material is available at *Brain* online.

References

Belostotsky R, Ben-Shalom E, Rinat C, Becker-Cohen R, Feinsten S, Zeligson S, et al. Mutations in the mitochondrial seryltRNA synthetase cause hyperuricemia, pulmonary hypertension, renal failure in infancy and alkalosis, HUPRA syndrome. Am J Hum Genet 2011; 88: 193–200.

Bugiani M, Invernizzi F, Alberio S, Briem E, Lamantea E, Carrara F, et al. Clinical and molecular findings in children with complex I deficiency. Biochim Biophys Acta 2004; 1659: 136–47.

Edvardson S, Shaag A, Kolesnikova O, Gomori JM, Tarassov I, Einbinder T, et al. Deleterious mutation in the mitochondrial arginyl-transfer RNA synthetase gene is associated with pontocerebellar hypoplasia. Am J Hum Genet 2007; 81: 857–862.

Ghezzi D, Zeviani M. Mitochondrial disorders: nuclear gene mutations. Encyclopedia of Life Sciences (ELS). Chichester: John Wiley & Sons, Ltd; 2011.

Götz A, Tyynismaa H, Euro L, Ellonen P, Hyötyläinen T, Ojala T, et al. Exome sequencing identifies mitochondrial alanyl-tRNA synthetase mutations in infantile mitochondrial cardiomyopathy. Am J Hum Genet 2011; 88: 635–42.

Haack TB, Danhauser K, Haberberger B, Hoser J, Strecker V, Boehm D, et al. Exome sequencing 348 identifies ACAD9 mutations as a cause of complex I deficiency. Nat Genet 2010; 42: 1131–4.

Heckmatt JZ, Dubowitz V. Needle biopsy of skeletal muscle. Muscle Nerve 1984; 7: 594.

Pierce SB, Chisholm KM, Lynch ED, Lee MK, Walsh T, Opitz JM, et al. Mutations in mitochondrial histidyl tRNA synthetase HARS2 cause ovarian dysgenesis and sensorineural hearing loss of Perrault syndrome. Proc Natl Acad Sci USA 2011; 108: 6543–8.

Riley LG, Cooper S, Hickey P, Rudinger-Tirion J, McKenzie M, Compton A, et al. Mutation of the mitochondrial tyrosyl-tRNA synthetase gene, YARS2, causes myopathy, lactic acidosis, and sideroblastic anemia—MLASA syndrome. Am J Hum Genet 2010; 87: 52–9.

Rötig A. Human diseases with impaired mitochondrial protein synthesis. Biochim Biophys Acta 2011; 1807: 1198–205.

Scheper GC, van der Klok T, van Andel RJ, van Berkel CG, Sissler M, Smet J, et al. Mitochondrial aspartyl-tRNA synthetase deficiency causes leukoencephalopathy with brain stem and spinal cord involvement and lactate elevation. Nat Genet 2007; 39: 534–9.

Sciacco M, Bonilla E. Cytochemistry and immunocytochemistry of mitochondria in tissue sections. Methods Enzymol 1996; 264: 509–21.

Steenweg ME, Vanderver A, Ceulemans B, Prabhakar P, Régals L, Fattal-Valevski A, et al. Novel infantile-onset leukoencephalopathy with high lactate and slow improvement. Arch Neurol 2012 (in press). Epub ahead of print, doi:10.1001/archneurol.2011.1048.

Van der Knaap MS, Breiter SN, Naidu S, Hart AAM, Valk J. Defining and categorizing leukoencephalopathies of unknown origin: MR imaging approach. Radiology 1999; 213: 121–33.

Wu M, Neilson A, Swift AL, Moran R, Tamagnine J, Parslow D, et al. Multiparameter metabolic analysis reveals a close link between attenuated mitochondrial bioenergetic function and enhanced glycolysis dependency in human tumor cells. Am J Physiol Cell Physiol 2007; 292: C125–36.